

## Molecular modelling of acarviosine, the pseudo-disaccharide moiety of acarbose, and other inhibitors of alpha-amylases\*

Eric Raimbaud<sup>†</sup>, Alain Buléon, and Serge Pérez<sup>‡</sup>

*Laboratoire de Physicochimie des Macromolécules, Institut National de la Recherche Agronomique, B.P. 527, 44026 Nantes (France)*

(Received June 13th, 1991; accepted December 28th, 1991)

### ABSTRACT

Acarbose and its homologs inhibit  $\alpha$ -D-glucosidases, particularly alpha-amylases. These homologs have the same core, the pseudo-disaccharide acarviosine, linked to various numbers of glucose residues. The conformations of (*R*)- and (*S*)-acarviosine have been analysed. The potential energy maps, obtained by molecular mechanics calculations, show that acarviosine is flexible and has several important minima. One low-energy form is close to the shape assumed by the acarviosine moiety when acarbose is adsorbed on the surface of glycogen phosphorylase. Another likely conformation is the same as that inferred from n.m.r. data and HSEA calculations. The results reconcile those conflicting reports. Molecular modelling of other inhibitors of alpha-amylases, such as 4-thiomaltose and moranoline, shows that these pseudo-disaccharides can fill similar volumes of conformational space.

### INTRODUCTION

The discovery that microbial secondary metabolites can inhibit  $\alpha$ -D-glucosidases and alpha-amylases has stimulated many studies<sup>1</sup>. In particular, they have aroused interest as potential agents for the treatment of such metabolic diseases as diabetes, and such studies have given a better understanding of the mechanism of action of glycohydrolases. These inhibitors are thought to be active site-directed substrates, and the specific amino acids involved in the interactions are known.

Several pseudo-oligosaccharide inhibitors of  $\alpha$ -D-glucosidases and alpha-amylases, such as acarbose and its homologues isolated from cultures of micro-organisms, have, as a common fragment, the pseudo-disaccharide acarviosine. This fragment, essential for inhibitory action, consists of a conduritol residue  $\alpha$ -(1→4)-linked to a 4-amino-4,6-dideoxy-D-glucose residue.

<sup>1</sup>H-N.m.r. and n.O.e. data<sup>2</sup> for acarbose and acarviosine, combined with HSEA calculations, have been interpreted in terms of a single preferred conformation. On the other hand, the crystal structure<sup>3</sup> of glycogen phosphorylase bound to acarbose re-

\* Dedicated to Professor David Manners.

<sup>†</sup> Present address: U.C.B. s.a., Chemin du Foriest, 1420 Braine L'Alleud, Belgium.

<sup>‡</sup> Author for correspondence.

vealed a conformation in the solid state which was different from that derived from HSEA calculations. Therefore, it might be thought that the enzyme stabilises a high-energy conformation of its inhibitor.

In order to relate the structure of molecules to their physical and biological properties, accurate representations of conformational space are needed. Although simple modelling algorithms can give useful approximations, elaborate, relaxed-residue molecular mechanics methods have now been reported for disaccharides<sup>4-8</sup>. These reports argue that all internal co-ordinates must be relaxed in order to obtain correct energy surfaces. We now report studies of the conformational space available to acarviosine and other alpha-amylase inhibitors by the relaxed-residue method.

## EXPERIMENTAL

**Nomenclature.** — The inter-residue linkage of (*S*)- and (*R*)-acarviosine (methyl 4,6-dideoxy-4-[[[(1*S*)-(1,4,6/5)-4,5,6- trihydroxy-3-hydroxymethyl-2-cyclohexen-1-yl]-amino]- $\alpha$ -D-glucopyranoside and the 1*R*-isomer, respectively) were analysed. The *R* and *S* descriptors are used to describe the absolute configuration of the nitrogen atom. The molecule consists of a hydroxymethylconduritol residue  $\alpha$ -(1 $\rightarrow$ 4)-linked to a 4-amino-4,6-dideoxy-D-glucopyranose residue.

Fig. 1 shows the atoms and the torsion angles of interest. The atoms of the hydroxymethylconduritol residue and the 4-amino-4,6-dideoxy-D-glucopyranose resi-

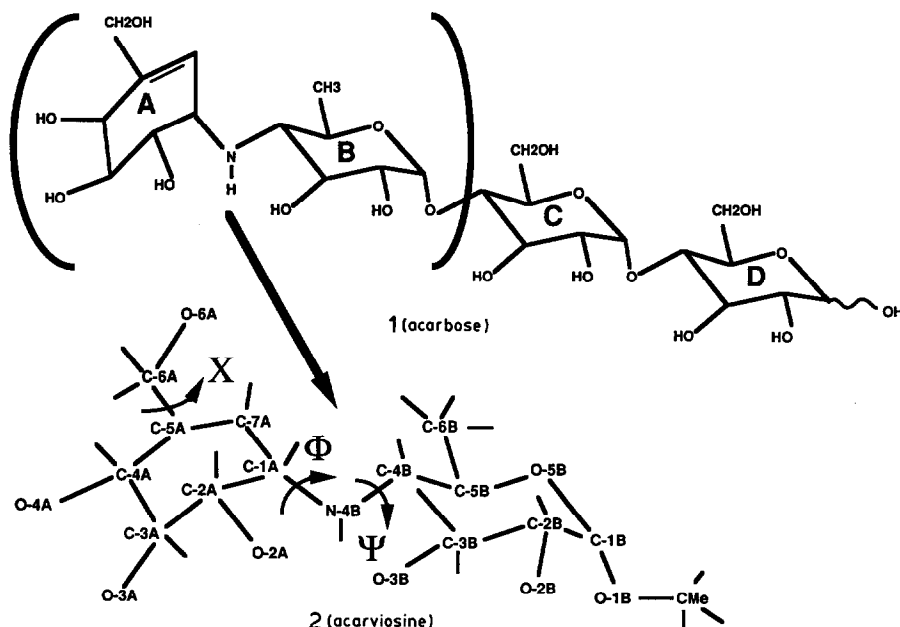


Fig. 1. Schematic representation of acarbose (1) along with the atom labelling and the torsional angles of interest of acarviosine (2).

due are designated A and B, respectively. The recommendations proposed<sup>9</sup> by the IUPAC have been used. The conformation at the glycosidic linkage is described by the torsion angles  $\Phi$  C-7A-C-1A-N-4B-C-4B or  $\Phi_H$  H-1A-C-1A-N-4B-C-4B, and  $\Psi$  C-1A-N-4B-C-4B-C-5B or  $\Psi_H$  C-1A-N-4B-C-4B-H-4b. The exocyclic torsion angle X (C-7A-C-5A-C-6A-O-6A) defines the orientation of the hydroxymethyl group of the conduritol moiety. The two prochiral methylene hydrogen atoms at C-6A can be differentiated using the rule proposed by Hanson<sup>10</sup>.

*Energy calculations.* — (a) *For acarviosine.* All calculations were done on Digital workstations at the I.N.R.A. Research Centre (Nantes). The allowed conformations and their energies were determined first with a rigid-residue method and then with a relaxed-residue modelling program. For each method, the starting geometries of the pseudo-disaccharides were fully optimised models. The preferred orientations of the hydroxymethylconduritol residue were investigated by systematically rotating the torsion angle X over the whole range by increments of 20°. For each orientation, the conformation of the conduritol moiety was fully optimised through molecular mechanics calculations.

(i) *Rigid-map calculations.* The computer program PFOS<sup>11,12</sup> was used in which the conformational energy is the sum of the contributions from van der Waals forces, torsional parameters, and inter-residue hydrogen bonding. Since the ring of the conduritol moiety has no heteroatoms, there is no exo-anomeric effect. The ring geometries are invariant, and hydroxylic hydrogen atoms were not used. A valence angle  $\tau$  of 114° was used that was taken from a geometry optimisation<sup>13</sup> by the semi-empirical quantum chemical method PCIO<sup>14</sup>. Altogether, six starting models were used: the two enantiomers, each with the three orientations of the hydroxymethyl group.  $\Phi$  and  $\Psi$  were stepped from -180° to 180° in increments of 5°. At each point, the energy was calculated with and without contributions from hydrogen bonding.

(ii) *Relaxed-residue calculations.* The MMP2(85) program<sup>15,16</sup> was used, for which useful minor changes have already been described<sup>17</sup>. Lone pairs of electrons on the oxygen and nitrogen atoms were added with a local program. Starting geometries were optimised structures from each of the local minima in the rigid-residue maps. The orientations of the hydroxymethyl groups were also tried. Hydroxylic hydrogen atoms were added in the clockwise and counter-clockwise orientations<sup>17</sup>. The changed MMP2(85) program has a new dihedral driver option that allows each optimisation to start with the same set of relative co-ordinates within the residues. With the standard driver -1 option, MMP2(85) starts each optimisation with the results of the previous optimisation. The standard driver causes any structural changes that occur during the optimisation of high-energy structures, such as rotated hydroxyl groups, to be passed to the next optimisation.

The energies were calculated on a 20° × 20° grid of  $\Phi$  and  $\Psi$ . At each grid point, the internal co-ordinates, except the linkage torsion angles, were fully optimised. Like the other atoms, the hydroxymethyl groups were allowed to adjust. However, the energy barriers separating the staggered positions are so high that the hydroxymethyl groups stayed in their original general orientations during optimisation, regardless of  $\Phi$  and  $\Psi$ .

(b) *For other alpha-amylase inhibitors.* Apart from the acarviosine unit, other disaccharides or pseudo-disaccharides, such as 4-thiomaltose or 4-*O*- $\alpha$ -D-glucopyranosyl-*N*-methylmoranoline (moranoline), inhibit alpha-amylases. These molecules, for which crystal structures have been reported<sup>18,19</sup>, were also submitted to a conformational analysis making use of the rigid-residue approach, with the PFOS computer program. Since these molecules contain heteroatoms, the stabilising influence of the exo-anomeric effect had to be included. The valence angle at the inter-residue linkage was set to 100.3° and to 120.8° for 4-thiomaltose<sup>18</sup> and moranoline<sup>19</sup>, respectively. For the sake of comparison<sup>20</sup>, the results from a conformational analysis of maltose have been incorporated.

Flexible fits between low-energy conformations of two or more molecules were performed using the multifit option of the SYBYL package<sup>21</sup> and selected atoms together with spring strengths between the fitted points. A term of the form

$$E_{\text{mult}} = k_i^s d_i^2$$

was included, which reflects the quality of fit, and where  $k_i^s$  is a spring constant (kcal/mol Å<sup>2</sup>) and  $d_i$  is the distance between the atom and the reference point. The co-ordinates of the reference point are the arithmetic means of the co-ordinates of the atoms to be superimposed. The purpose of this term is to force atoms of different molecules to occupy the same place, whilst simultaneously adjusting the geometry of each molecule in order to relieve any strain and maintain a low energy.

## RESULTS AND DISCUSSION

*Stereochemical features of the hydroxymethylconduritol residue.* — A representation of the conduritol moiety in one of its low energy conformations is shown in Fig. 2. The bond distances and angles along with some torsional angles of interest have been deposited\*. The calculations established that the conformation of the ring is the half-chair <sup>3</sup>H<sub>2</sub>, as indicated by the three puckering parameters ( $q = 0.514$ ,  $\theta = 131^\circ$ , and  $\phi_2 = 254^\circ$ ) according to the Cremer and Pople definition<sup>22</sup>. The stable arrangements of the hydroxymethyl group fall into the three low-energy conformations depicted in Fig. 3.

*Conformation about the N-linkage.* — The three relaxed maps calculated for the (*S*) and (*R*) isomers represented in Fig. 4 were obtained with a clockwise orientation of the hydrogen atoms of the secondary hydroxyl groups, which always yielded the lowest energy. These  $\Phi, \Psi$  maps represent multidimensional space, since the conformation is no longer a function of two variables. For each isomer, the three maps are not strikingly different since the orientations of the hydroxymethyl group do not have a major influence on the energy. However, for the (*R*) isomer, the minimum located at  $\Phi = 40^\circ$ ,  $\Psi = 50^\circ$  disappears when the torsion angle X is  $-10^\circ$ . For each of these relaxed maps, the geometry of each minima was refined completely, including the relief of the

\* These data can be obtained from Elsevier Science Publishers BV, BBA Data Deposition, P.O. Box 1527, Amsterdam, The Netherlands. Reference should be made to No BBA/DD/499/ *Carbohydr. Res.*, 227 (1992) 351–363.

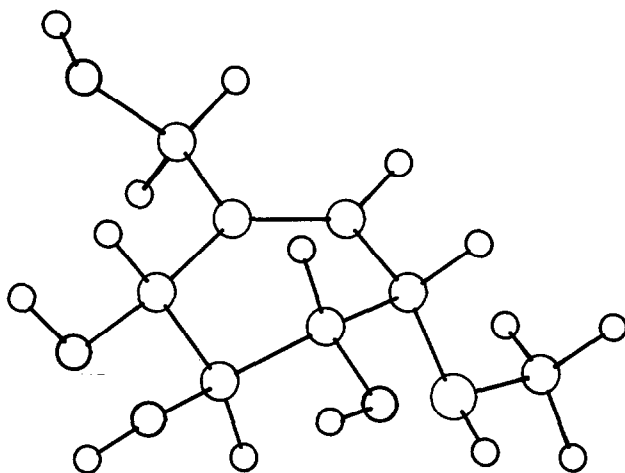


Fig. 2. Representation of the hydroxymethylconduritol residue A in Fig. 1 in its low-energy conformation.

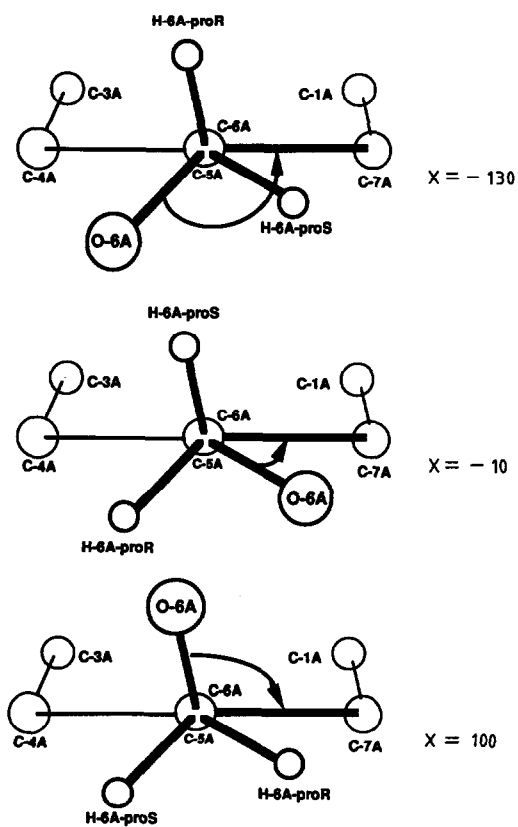


Fig. 3. Schematic representation of the three stable conformations of the hydroxymethyl group of the conduritol moiety (see Fig. 1).

TABLE I

Conformational features and energy values of the low-energy minima after complete energy minimisation through MM285<sup>a</sup>

Name	$\Phi$ (°)	$\Psi$ (°)	$\chi$ (°)	$\tau$ (°)	$\Delta E$ with hydrogen bond (kcal/mol)	$\Phi_H$ (°)	$\Psi_H$ (°)	H-bond length (nm)	H-bonded atoms
<b>(S)-Acarviosine</b>									
Sr1	80.1	-139.9	-129.7	114.1	0.00	-39.9	-19.9		
Sr3	57.6	45.1	-129.3	118.9	0.11	-62.4	165.1		
Sr4	142.9	-98.4	-132.0	115.9	3.97	22.9	21.6	0.302	O-2A-O-3B
Sr1	80.1	-139.9	-7.8	114.0	2.47	-39.9	-19.9		
Sr3	57.2	46.1	-5.3	118.9	2.57	-62.8	166.1		
Sr4	159.2	-99.3	-10.9	116.7	5.84	39.2	20.7	0.321	O-2A-O-3B
Sr1	80.2	-139.9	106.9	113.8	0.89	-39.8	-19.9		
Sr3	59.4	46.2	106.9	118.7	0.29	-60.6	166.2		
Sr4	158.9	-98.6	107.8	116.8	4.08	38.9	21.4	0.320	O-2A-O-3B
<b>(R)-Acarviosine</b>									
Rr1	79.5	-139.7	-130.1	114.4	0.00	-40.5	-19.7		
Rr2	149.2	-95.3	-130.3	116.1	1.34	29.2	24.7	0.313	O-2A-O-3B
Rr3	100.3	73.9	-129.3	116.9	2.28	-19.7	-166.1		
Rr4	42.3	53.3	-131.9	119.7	2.91	-77.7	173.3		
Rr5	-79.9	-159.2	-129.3	120.9	4.70	160.1	-39.2		
Rr1	80.2	-139.4	-7.0	114.2	2.23	-39.8	-19.4		
Rr2	142.9	-93.4	-9.0	115.8	3.34	22.9	26.6	0.314	O-2A-O-3B
Rr3	90.8	69.5	-1.3	117.6	3.73	-29.2	-170.5		
Rr5	-81.5	-151.7	-6.8	120.2	6.43	158.5	-31.7		
Rr1	79.6	-139.7	105.1	114.1	0.56	-40.4	-19.7		
Rr2	142.7	-93.1	105.0	115.6	1.87	22.7	146.9	0.314	O-2A-O-3B
Rr3	81.0	59.7	103.6	118.6	2.56	-39.0	-60.3		
Rr4	46.5	52.7	107.0	119.4	2.40	-73.5	-67.3		
Rr5	-79.4	-159.5	103.8	120.9	5.10	160.6	80.5		

<sup>a</sup> The most stable conformation for (S)-acarviosine is 0.83 kcal/mol lower in energy than its counterpart for (R)-acarviosine.

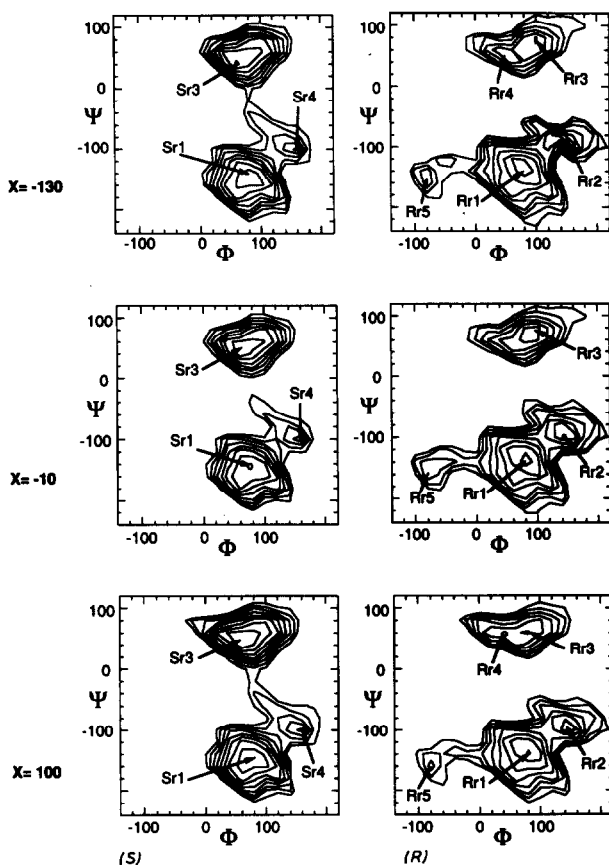


Fig. 4. Relaxed potential-energy surfaces of acarviosine, for each of the low-energy orientations of the hydroxymethyl groups. Isoenergy contours are drawn with interpolation of 1 kcal/mol above the minimum of each map.

constraint on  $\Phi$  and  $\Psi$ . The final geometries and energy values of these minima are listed in Table I and the eight where  $X$  is  $-10^\circ$  are represented in Fig. 5. The lowest minimum of the (*S*)-acarviosine in Table I is 0.83 kcal/mol above the lowest for (*R*)-acarviosine. Hydrogen bonding may occur at  $\Phi = 160^\circ$  and  $\Psi = -100^\circ$  for (*S*)-acarviosine since the distance between O-2A and O-3B is 0.32 nm. For (*R*)-acarviosine, there is one hydrogen at  $\Phi = 150^\circ$ ,  $\Psi = -95^\circ$  for a distance between the same atoms of 0.31 nm.

An adiabatic map which represents the synthesis of the three individual relaxed potential-energy surfaces was constructed for each isomer (Fig. 6). In these maps, each point of the grid corresponds to the lowest-energy conformation. All three partially relaxed surfaces contribute to the adiabatic map. These maps must be used carefully because they represent a two-dimensional projection of a more complicated hyperspace. The results obtained indicate the need to consider the absolute configuration at the nitrogen atom in conformational analyses of *N*-glycosyl compounds.

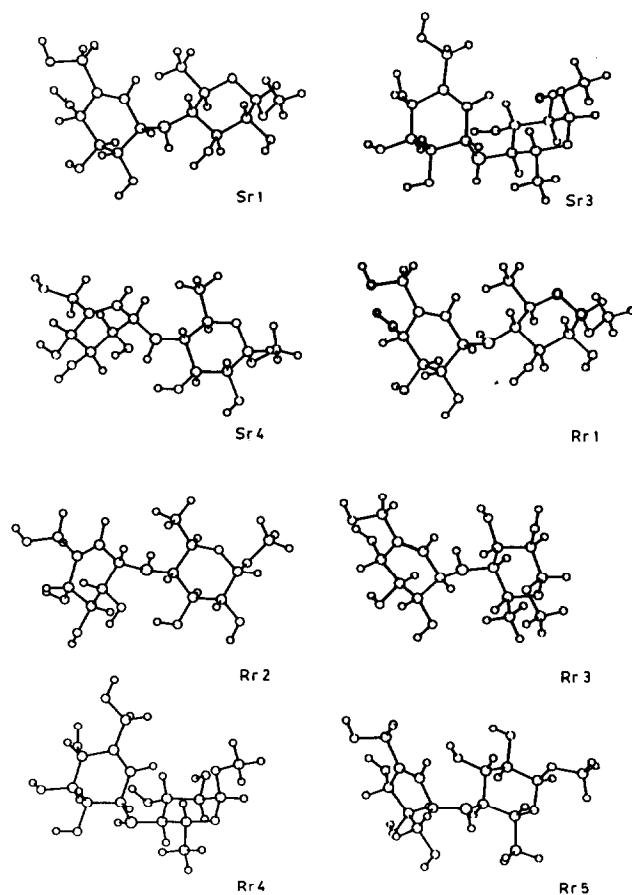


Fig. 5. Molecular representations of the low-energy conformations of the acarviosine molecule. The minima chosen have the hydroxymethyl group in the same orientation with  $X = -10^\circ$ .

*Comparison with experimental results.* — The three-dimensional structure<sup>3</sup> of acarbose bound to glycogen phosphorylase permits comparison between the predicted conformations of the acarviosine moiety and that observed in the solid state. It has been emphasised that the conduritol moiety makes no contacts with the protein and is less well ordered than the remaining sugars. For these reasons, errors in the conformation angles have been estimated to be of the order of a few degrees. The characteristic features are as follows: the conduritol moiety remains in the  $^3H_2$  conformation, the torsion angle  $X$  of the hydroxymethyl group is  $34.8^\circ$ , at the  $N$ -linked junction the magnitude of the valence angle  $\tau$  is  $111.7^\circ$ , and the torsion angles are  $\Phi = 117.2^\circ$  and  $\Psi = -98.8^\circ$ . Consequently, the occurrence of an inter-residue hydrogen bond between O-2A and O-3B (0.309 nm) has been postulated. This observed conformation falls into the low-energy domains of the (*R*) and (*S*) enantiomers, and it is within  $20^\circ$  from the low-energy conformers Sr4 or Rr2 (Fig. 5). Therefore, it is concluded that the binding of



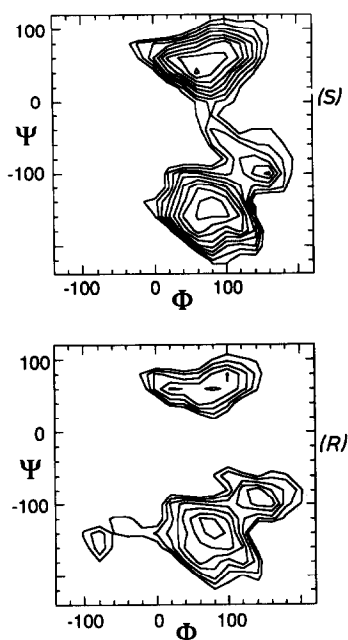


Fig. 6. Adiabatic relaxed potential-energy surface of the acarviosine molecule. This map was created from the three previous maps by plotting for each conformation that with the lowest energy among the three examined. Isoenergy contours are drawn by interpolation of 1 kcal/mol above the minimum.

acarbose to the protein surface does not stabilise an alternative high-energy conformation. The agreement between the calculated and the observed conformations is excellent.

The solid-state conformation of the acarviosine moiety<sup>3</sup> was reported not to be consistent with that proposed<sup>2</sup> for its solution behaviour, as inferred from high-resolution n.m.r. spectroscopy and HSEA calculations. It was concluded that, in solution, the conformation of the conduritol ring is <sup>3</sup>H<sub>2</sub>, and that there is one preferred conformation about the *N*-linkage having values centered at  $\Phi = 83.1^\circ$ ,  $\Psi = -139.6^\circ$ , and  $\tau = 108^\circ$ . Such a conformation closely corresponds to the low-energy conformers S1, R1, Sr1, or Rr1.

From this study, as well as from other comparisons between relaxed maps and rigid maps, it appears that the only way a rigid-residue approach can be useful is to consider all low-energy minima, even isolated ones, within 10 kcal/mol.

*Molecular modelling of other amylase inhibitors.* — The rigid potential-energy surfaces calculated for (*R*)-acarviosine, 4-thiomaltose, and moranoline are represented on Fig. 7, together with that for maltose. Despite some expected differences between the four maps, marked similarities appear, such as the occurrence of a large low-energy domain which encompasses almost the same region on the  $\Phi, \Psi$  map, and the occurrence of an island centered at  $\Phi = 80^\circ$ , and  $\Psi = 70^\circ$ . Also, the low-energy conformers occur

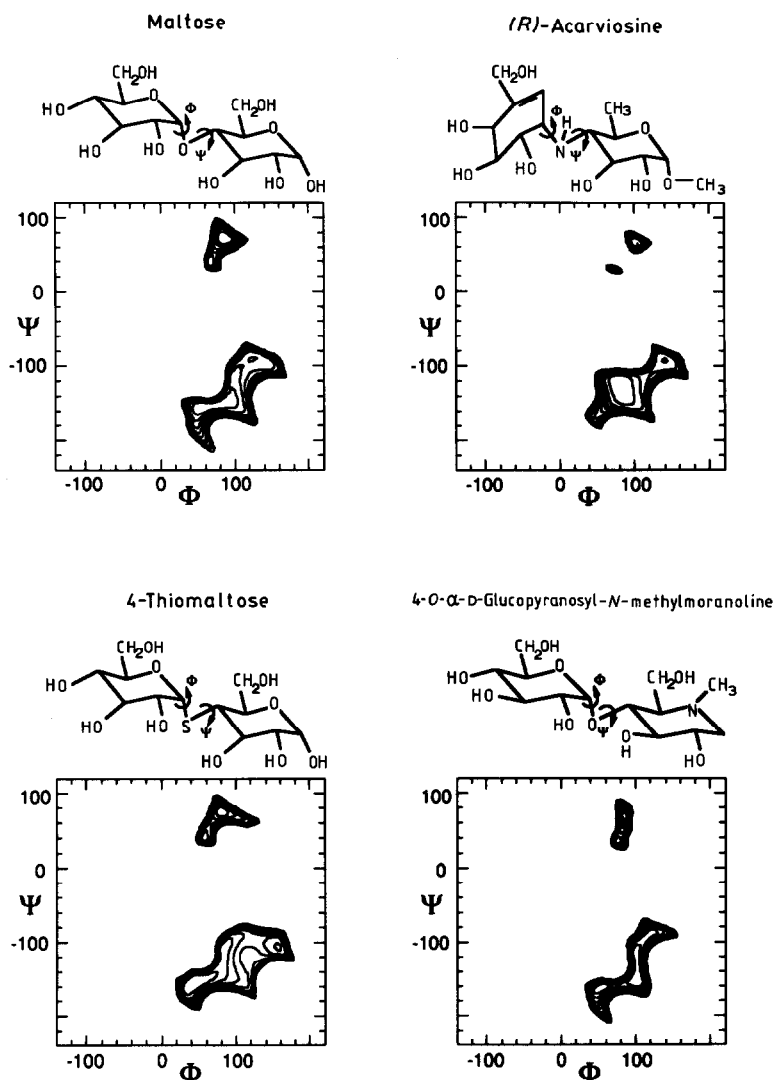


Fig. 7. 2D Rigid iso-energy maps ( $\Phi, \Psi$ ) computed for maltose, (*R*)-acarviosine, 4-thiomaltose, and 4-*O*- $\alpha$ -D-glucopyranosyl-*N*-methylmoranolamine.

at similar  $\Phi, \Psi$  values. For each molecule, three representatives having the lowest energy were selected, *i.e.*, maltose  $\Phi = 80^\circ$ ,  $\Psi = -150^\circ$  (F1);  $\Phi = 120^\circ$ ,  $\Psi = -100^\circ$  (F2);  $\Phi = 80^\circ$ ,  $\Psi = 70^\circ$  (F3); (*R*)-acarviosine,  $\Phi = 80^\circ$ ,  $\Psi = -140^\circ$  (F1);  $\Phi = 140^\circ$ ,  $\Psi = -100^\circ$  (F2);  $\Phi = 100^\circ$ ,  $\Psi = 70^\circ$  (F3); 4-thiomaltose,  $\Phi = 60^\circ$ ,  $\Psi = -150^\circ$  (F1);  $\Phi = 150^\circ$ ,  $\Psi = -110^\circ$  (F2);  $\Phi = 80^\circ$ ,  $\Psi = 70^\circ$  (F3); moranolamine,  $\Phi = 60^\circ$ ,  $\Psi = -160^\circ$  (F1);  $\Phi = 120^\circ$ ,  $\Psi = -90^\circ$  (F2);  $\Phi = 85^\circ$ ,  $\Psi = 70^\circ$  (F3). For a given family, the

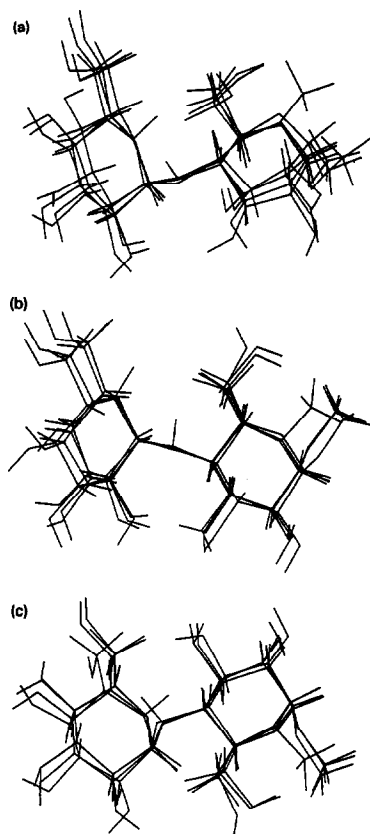


Fig. 8. Superimposition of the best fitted conformations of maltose, (*R*)-acarviosine, 4-thiomaltose, and 4-*O*- $\alpha$ -D-glucopyranosyl-*N*-methylmoranolone: (a) F1, (b) F2, (c) F3 (see Table II).

similarity or lack of similarity between these conformers was investigated. The results of the fit procedures are listed in Table II. For each pair of conformers, two root-mean-square values are given; one was calculated using the five atoms that define  $\Phi$  and  $\Psi$  torsional angles, and the other using the 12 non-hydrogen atoms plus the junction atom of each molecule. The highest r.m.s. value is 0.03 nm. For each family, the representation of the best-fitted conformations have been superimposed and they are shown in Fig. 8. From the present work, it was expected that significant differences between some regions of the conformational space which is shared by the four molecules would be detected. It is clear that they all share a common conformational space and that, within it, the low-energy conformations resemble each other to the point where they can be superimposed almost perfectly; this may help to explain why these inhibitors interact with the catalytic site of  $\alpha$ -amylases.

TABLE II

Results of the flexible fits between the low-energy conformers of maltose, acarviosine, 4-thiomaltose, and moranoline<sup>a</sup>

Molecule	Minima Starting values (°)		Minima Final values (°)		R.m.s. (nm) <sup>b</sup>	R.m.s. (nm) <sup>c</sup>
	Φ	Ψ	Φ	Ψ		
Maltose (F1)	80	-150	72.6	-155.6		
Acarviosine	80	-150	77.2	-144.9	0.0096	0.0203
4-Thiomaltose	60	-150	62.4	-153.4	0.0191	0.0266
Moranoline	60	-160	61.1	-159.1	0.0061	0.0205
Maltose (F2)	120	-100	136.7	-100.7		
Acarviosine	140	-100	137.9	-95.3	0.0068	0.0125
4-Thiomaltose	150	-110	137.3	-99.5	0.0188	0.0331
Moranoline	120	-90	130.9	-98.8	0.0035	0.0094
Maltose (F3)	80	70	78.3	75.6		
Acarviosine	100	70	89.0	68.7	0.0100	0.0216
4-Thiomaltose	80	70	79.9	76.1	0.0179	0.0231
Moranoline	85	70	78.6	76.0	0.0007	0.0038

<sup>a</sup> For a given family, the conformation of the three inhibitors was multifitted to that of maltose. <sup>b</sup> Calculated using the five atoms defining the  $\Phi$  and  $\Psi$  torsional angles. <sup>c</sup> Calculated using the 12 non-hydrogen atoms plus the junction atom.

## ACKNOWLEDGMENT

DuPont de Nemours is thanked for a grant (to E.R.).

## REFERENCES

- 1 E. Truscheit, W. Frommer, B. Junge, L. Müller, D. D. Schmidt, and W. Wingender, *Angew. Chem. Int. Ed. Engl.*, 20 (1981) 744-761.
- 2 K. Bock and H. Pedersen, *Carbohydr. Res.*, 132 (1984) 142-149.
- 3 E. J. Goldsmith, R. J. Fletterick, and S. G. Withers, *J. Biol. Chem.*, 262 (1987) 1449-1455.
- 4 J. Jimenez-Barbero, O. Noble, C. Pfeffer, and S. Pérez, *Nouv. J. Chim.*, 12 (1988) 941-946.
- 5 A. D. French, *Biopolymers*, 27 (1988) 1519-1525.
- 6 S. N. Ha, L. J. Madsen, and J. W. Brady, *Biopolymers*, 27 (1988) 1927-1952.
- 7 V. Tran, A. Buléon, A. Imberty, and S. Pérez, *Biopolymers*, 28 (1989), 679-690.
- 8 A. Imberty, V. Tran, and S. Pérez, *J. Comput. Chem.*, 11 (1989) 205-216.
- 9 IUPAC-IUB, Commission on Biological Nomenclature, *Arch. Biochem. Biophys.*, 145 (1971) 405-421.
- 10 K. R. Hanson, *J. Am. Chem. Soc.*, 88 (1966) 2731-2742.
- 11 S. Pérez, DSc Thesis, University of Grenoble, France, 1978.
- 12 I. Tvaroska and S. Pérez, *Carbohydr. Res.*, 149 (1986) 389-410.
- 13 T. Kozar and I. Tvaroska, *Biopolymers*, 29 (1991) 1531-1539.
- 14 S. Diner, J. P. Malrieu, F. Jordan, and M. Gilbert, *Theor. Chim. Acta*, 15 (1969) 100-110.
- 15 N. L. Allinger, *J. Am. Chem. Soc.*, 99 (1977) 8127-8134.
- 16 Quantum Chemistry Program Exchange, Department of Chemistry, Indiana State University, Bloomington, IN 47901, U.S.A.
- 17 A. D. French, V. Tran, and S. Pérez, *ACS Symp. Ser.*, 430 (1990) 191-212.

- 18 S. Pérez and C. Vergelati, *Acta Crystallogr., Sect. B*, 40 (1984) 294–299.
- 19 Y. Ezure, Y. Yoshikuni, N. Ojima, and M. Sugiyama, *Acta Crystallogr., Sect. C*, 43 (1987) 1809–1811.
- 20 S. Pérez and C. Vergelati, *Polym. Bull.*, 17 (1987) 141–148.
- 21 SYBYL, Tripos Associate Inc. (Evans and Sutherland, St. Louis, MO, U.S.A.).
- 22 D. Cremer and J. A. Pople, *J. Am. Chem. Soc.*, 97 (1975) 1354–1358.